Semiconductor Science and Technology

LETTER

# Charge-neutral nonlocal response in superconductor-InAs nanowire hybrid devices

To cite this article: A O Denisov *et al* 2021 *Semicond. Sci. Technol.* **36** 09LT04





Letters

IOP Publishing

Semiconductor Science and Technology

Semicond. Sci. Technol. **36** (2021) 09LT04 (6pp)

https://doi.org/10.1088/1361-6641/ac187b

Letter

# Charge-neutral nonlocal response in superconductor-InAs nanowire hybrid devices

**A O Denisov[1,2], A V Bubis[3,1], S U Piatrusha[1], N A Titova[4], A G Nasibulin[3,5], J Becker[6], J Treu[6], D Ruhstorfer[6], G Koblmüller[6], E S Tikhonov[1] and V S Khrapai[1,*]**

[1] Institute of Solid State Physics, Russian Academy of Sciences, 142432 Chernogolovka, Russia
[2] Department of Physics, Princeton University, Princeton, NJ 08544, United States of America
[3] Skolkovo Institute of Science and Technology, Nobel street 3, 121205 Moscow, Russia
[4] Moscow Pedagogical State University, 29 Malaya Pirogovskaya St, 119435 Moscow, Russia
[5] Aalto University, P.O. Box 16100, 00076 Aalto, Finland
[6] Walter Schottky Institut, Physik Department, and Center for Nanotechnology and Nanomaterials, Technische Universität München, Am Coulombwall 4, 85748 Garching, Germany

E-mail: dick@issp.ac.ru

Received 14 June 2021, revised 15 July 2021
Accepted for publication 28 July 2021
Published 6 August 2021

**Abstract**

Nonlocal quasiparticle transport in normal-superconductor-normal (NSN) hybrid structures probes sub-gap states in the proximity region and is especially attractive in the context of Majorana research. Conductance measurement provides only partial information about nonlocal response composed from both electron-like and hole-like quasiparticle excitations. In this work, we show how a nonlocal shot noise measurement delivers a missing puzzle piece in NSN InAs nanowire-based devices. We demonstrate that in a trivial superconducting phase quasiparticle response is practically charge-neutral, dominated by the heat transport component with a thermal conductance being on the order of conductance quantum. This is qualitatively explained by numerous Andreev reflections of a diffusing quasiparticle, that makes its charge completely uncertain. Consistently, strong fluctuations and sign reversal are observed in the sub-gap nonlocal conductance, including occasional Andreev rectification signals. Our results prove conductance and noise as complementary measurements to characterize quasiparticle transport in superconducting proximity devices.

Supplementary material for this article is available online

Keywords: shot noise, Andreev reflection, non-local transport, hybrid devices, Majorana zero modes, thermal conductance

(Some figures may appear in colour only in the online journal)

Nonlocal conductance measurements [1] in semiconductor-superconductor proximity structures gain renewed interest in the context of Majorana research [2–8]. The key underlying idea is that the nonlocal signals can probe global sub-gap states characteristic of a true topological phase transition [9–11]. This is in contrast to a standard two-terminal conductance [12–14] sensitive to the states near the point where the current inflows in the proximity region. Recent experiments in three-terminal NSN nanowire-based

* Author to whom any correspondence should be addressed.

 

(NW-based) hybrid devices confirm conceptual power of the nonlocal conductance approach [15, 16].

Conductance measurement provides only partial information about quasiparticle non-equilibrium in proximity structures. A sub-gap quasiparticle entering the proximity region carries the electric charge, $q < 0$ for electron-like and $q > 0$ for hole-like quasiparticles, and the excitation energy $\varepsilon = |E| > 0$, where $E$ is the kinetic energy relative to the chemical potential of the superconductor. On its way, apart from possible normal scattering, a quasiparticle experiences a few Andreev reflections (ARs) from the superconducting lead [17, 18], each time inverting the $q$ but preserving the $\varepsilon$. Thereby, the AR mediates a coupling of the charge and heat (energy) transport components that is unique to proximity structures and does not occur in bulk superconductors [19, 20]. Thus, a full characterization of the non-equilibrium can be achieved by a measurement of both the electric and heat nonlocal conductances.

In this article, we investigate the nonlocal response in NSN InAs NW-based devices. We show that a quasiparticle non-equilibrium can be understood if the nonlocal conductance is accompanied by a shot noise measurement substituting the heat conductance measurement, that allows to separate the contributions of transmission processes involving even and odd number of the ARs. Experiments performed in a trivial superconducting phase demonstrate that quasiparticle transport is practically charge-neutral, so that the heat transport component dominates the nonlocal response in our devices. Our results prove shot noise as a valuable, complementary to conductance, tool to probe the sub-gap states in proximity structures.

We start the discussion from the energy diagram of the NSN NW-based hybrid structure in a nonlocal experiment sketched in figure 1(a). Consider the case of zero temperature $T = 0$ and negative bias voltage $V_1 < 0$ applied to the left normal terminal $N_1$. The superconductor and the right normal terminal $N_2$ are grounded, position of their chemical potential shown by the dashed line. Transmitted quasiparticles are distinguished by their energy relative to this chemical potential, $\varepsilon > 0$ for electrons and $-\varepsilon$ for holes. Inside the NW quasiparticles experience ARs from the S-lead and elastic normal scattering from disorder and possibly from the S/NW interface, inelastic scattering is absent [21]. The charge current $I_2$ and the heat current $J_2$ in the right lead read [22, 23]:

$$I_2 = -\frac{e^2}{h} V_1 \Sigma \mathcal{T}_-; \; J_2 = \frac{e^2}{2h} V_1^2 \Sigma \mathcal{T}_+; \; \mathcal{T}_\pm \equiv T_{21} \pm A_{21} \qquad (1)$$

where the positive direction for the electric current is from the lead into the scattering region and opposite for the heat current. $T_{21}$ and $A_{21}$ are the probabilities of transmission, respectively, preserving and changing a quasiparticle type, sometimes also called normal and crossed-Andreev transmission [6] and the sum over the eigenchannels is performed. Generally, the two transmission processes involve both the normal and Andreev scattering and are distinguished by the parity of the number of ARs involved. Processes with an even and odd number of ARs contribute, respectively, to $T_{21}$ and $A_{21}$. Equations (1) imply that a simultaneous measurement of the charge and heat

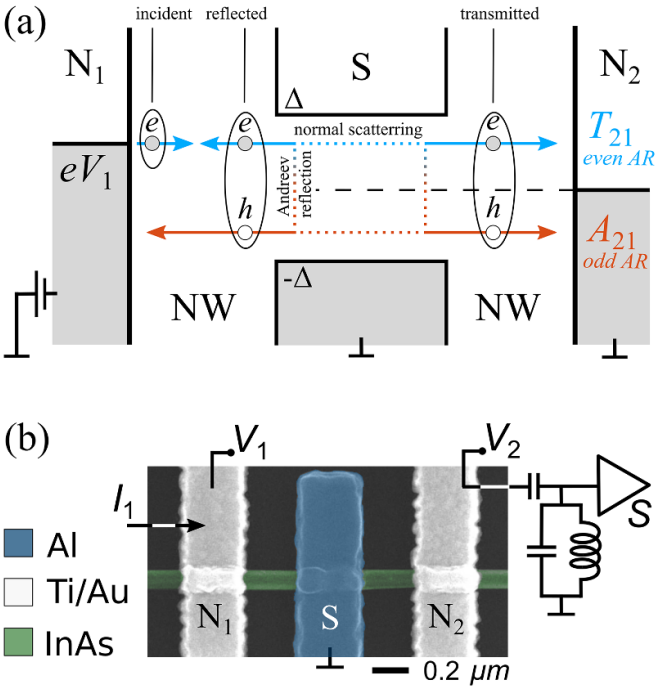


**Figure 1.** (a) Energy diagram of the NSN NW-based device. In this illustration, the left normal terminal $N_1$ is biased with voltage $V_1 < 0$, while the central S-terminal and the right $N_2$ terminal are grounded, their chemical potential shown by the dashed line. Depending on the number of Andreev reflections, the electron incident from $N_1$ can be transmitted towards $N_2$ as an electron ($e$) or hole ($h$) with probability $T_{21}$ or $A_{21}$ correspondingly. (b) Scanning electron microscope image of the NSN-II device (false color) and the shot-noise measurement scheme used in actual experiment. Voltages $V_1$ and $V_2$ that build up in response to the current bias $I_1$ are measured in a quasi-four-terminal configuration.

response permits an independent characterization of $T_{21}$ and $A_{21}$. Measurement of the heat transport is not an easy task [24–27] and we choose a different path in the present experiment. We perform a shot noise measurement in a nonlocal configuration [21, 28, 29], based on the findings of [11] briefly mentioned below.

The average charge $Q_2$ (in units of $e$) transmitted in one eigenchannel in an individual scattering event equals $\langle Q_2 \rangle = \mathcal{T}_-$. Its fluctuation is $\langle (\delta Q_2)^2 \rangle = \langle Q_2^2 \rangle - \langle Q_2 \rangle^2$, where $\langle Q_2^2 \rangle = \mathcal{T}_+$. Thus, in the spirit of [30], we obtain for the spectral density of the current noise in the right lead:

$$S_2 = \frac{2e^3}{h} |V_1| \Sigma \left( \mathcal{T}_+ - \mathcal{T}_-^2 \right), \qquad (2)$$

that contains $\mathcal{T}_+$ and can substitute $J_2$ in a nonlocal measurement. In the limit of suppressed AR $A_{21} \to 0$ equation (2) reduces to a familiar result in the normal case [31]. In this case, a nonlocal Fano factor defined as $F_{\rm nl} \equiv S_2 / 2e|I_2|$ is bounded by unity $F_{\rm nl} = 1 - T_{21} \leq 1$. In the opposite limit of $T_{21} = A_{21}$ the shot noise and the heat current remain finite, $S_2 \propto J_2$, whereas $I_2 = 0$. Here, the nonlocal quasiparticle response is charge-neutral and $F_{\rm nl} \to \infty$.

Equations (1) and (2) illustrate our main idea that nonlocal conductance $G_{21} \equiv \partial I_2 / \partial V_1$ and shot noise $S_2$ can

serve as two complementary electrical measurements required to fully characterize quasiparticle transport. We apply this paradigm to explore the nonlocal response in InAs NW-based NSN devices. The outline of the experiment is depicted in figure 1(b). A semiconducting InAs nanowire is equipped with an S terminal, made of Al, in the middle and two N terminals, made of Ti/Au bilayer, on the sides. In essence, this device represents two back-to-back N-NW-S junctions sharing the same S terminal. We study two similar devices, NSN-I and NSN-II, which have the width of S terminal equal to $w = 200$ nm and $w = 300$ nm, respectively. Note the absence of the plunger gates, typically used to define the quantum dots [32–34] or tunnel barriers [35] adjacent to the S-terminal. In addition, for all contacts in-situ Ar milling was applied before the evaporation in order to improve the semiconductor/metal interface quality. All of this enables better coupling of the sub-gap states to the normal conducting regions. As a result, the resistances of the individual N-NW-S junctions are mainly determined by disorder scattering rather than unintentional interface reflectivity. This is confirmed by smooth gate voltage characteristics and universal diffusive value of the shot noise Fano factor in the normal state, see the data of the related experiment in [36]. Throughout the experiments the S terminal is grounded, terminal $N_1$ is current biased. The terminal $N_2$ is DC floating throughout the experiment, which allows to access the differential resistances $R_{ij} \equiv \partial V_i/\partial I_j$ in a quasi-four-terminal configuration excluding the wiring contributions. The differential conductances are obtained by inverting the measured resistance matrix, see the Supplemental Material for the details (available online at stacks.iop.org/SST/36/09LT04/mmedia). In the present experiment, the non-diagonal elements are much smaller than the diagonal ones, so that approximate relations $G_{ii} \approx R_{ii}^{-1}$ and $G_{ij} \approx -R_{ij}(R_{11}R_{22})^{-1}$ hold within a few percent accuracy. Experiments are performed at bath temperatures of $T = 120$–$150$ mK unless stated otherwise.

Back-gate voltage ($V_g$) dependencies of the linear response diagonal conductances are shown in figure 2(a). $G_{ii}$ fall in the range of a few conductance quanta and exhibit a usual sublinear increase with $V_g$ accompanied by universal mesoscopic fluctuations. Standard procedure [37] gives a field-effect mobility of $\sim 300$ cm$^2$ (Vs)$^{-1}$ underestimated because of the field screening by contacts. Impact of a superconducting proximity effect on $G_{ii}$ is similar for both devices and all $V_g$ used, typical data shown in figure 2(b). In zero magnetic field $B$ a moderate zero-bias minimum is seen surrounded by maxima at $V = \pm\Delta/e$, where $\Delta = 180$ $\mu$eV is the Al superconducting gap, independently determined from the critical temperature, see Supplemental Material. In a uniform magnetic field of $B = 50$ mT obtained with a superconducting solenoid, oriented perpendicularly to the substrate and high enough to suppress the superconductivity the minimum weakens and the maxima disappear, whereas the above-gap conductance remains unchanged. Overall, this is a standard for coherent diffusive NS junctions re-entrant behaviour [38, 39], with a minor effect of the interface reflectivity and/or Coulomb effects [40].

The non-diagonal conductance probes quasiparticle transport via InAs-NW section underneath the S-terminal [4, 6, 7, 15, 16] and its bias dependence turns out much less

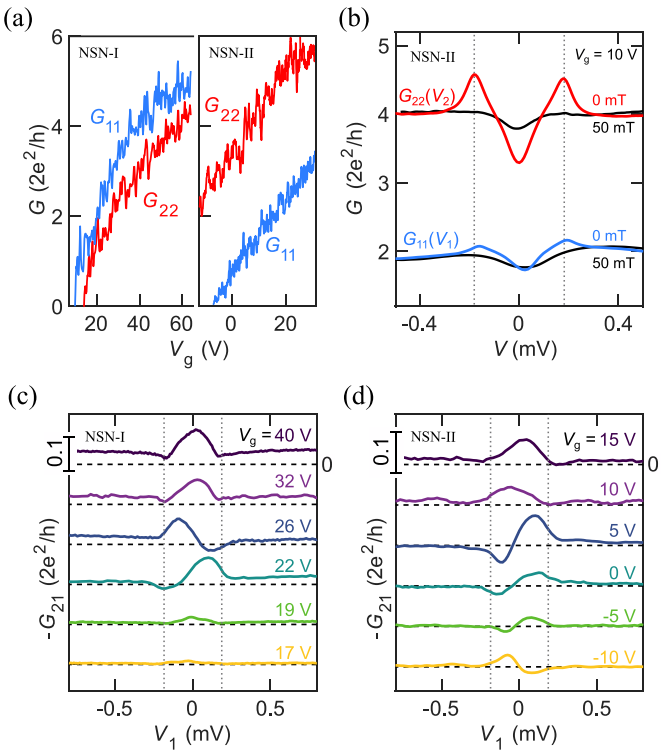


**Figure 2.** (a) Zero-bias diagonal conductances versus $V_g$ for both devices in zero magnetic field. (b) Diagonal differential conductance as a function of bias voltage in zero and high enough to suppress superconductivity magnetic fields. Dotted lines show position of the superconducting gap. (c) and (d) $B = 0$ nonlocal differential conductance as a function of $V_1$ for several $V_g$ values. The curves are vertically offset for clarity, with zero level shown by the dashed lines. Bars indicate the ordinate scale common for all $V_g$.

universal. In figures 2(c) and (d) we plot $-G_{21}$, having in mind that the negative sign corresponds to normal transmission. At sub-gap biases, very different behaviour of $-G_{21}$ can be observed depending on $V_g$, from almost symmetric with zero-bias maximum, see $V_g = 40$ V data in device NSN-I, to strongly anti-symmetric with sign inversion, see $V_g \leqslant 5$ V data in device NSN-II. By contrast, in the normal state $G_{21}$ is negative, featureless and consistent with a current transfer length of $\sim 100$ nm determined by a residual interface reflectivity, see the Supplemental Material. Figures 2(c) and (d) show that at sub-gap biases in the superconducting state $|G_{21}|$ strongly increases compared to its above-gap values, which is expected since quasiparticles are forbidden to enter the superconductor. The $G_{21}$ is much smaller than $e^2/h$ and occasionally changes sign, implying that $|\Sigma\mathcal{T}_-| \ll 1$ and fluctuates around zero as a function of energy and chemical potential. Below we present the nonlocal shot noise experiment that uncovers charge-neutral origin of the quasiparticle transport.

The layout of the shot noise measurement in a nonlocal configuration is sketched in figure 1(b). The current fluctuations are picked up at the floating terminal $N_2$ in response to the current between the biased terminal $N_1$ and the grounded S-terminal. Plotted as a function of $V_1$ all the data in both devices feature the same qualitative behaviour shown in

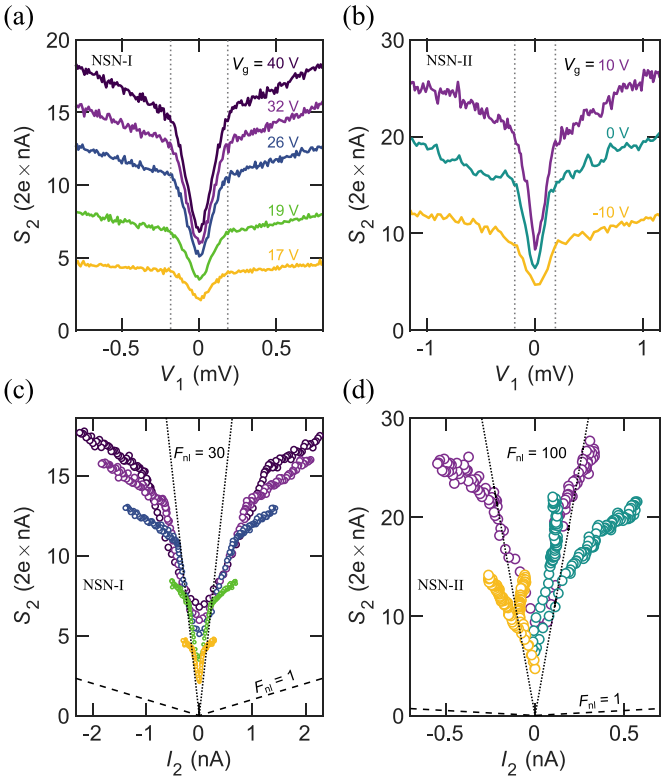


**Figure 3.** (a) and (b) Measured current noise spectral density in the right lead as a function of bias voltage on the left one. Dotted lines show positions of the superconducting gap. (c) and (d) Measured current noise spectral density in the right lead as a function of the nonlocal current $I_2$. Symbols have the same colour as the lines in panels (a) and (b) for the respective $V_g$. Guide lines with Fano-factor $F_{nl} = 1$ and $F_{nl} \gg 1$ are plotted as dashed and dotted lines correspondingly.

figures 3(a) and (b). The shot noise spectral density $S_2$ starts from the Johnson-Nyquist equilibrium value $4k_BTG_{22}$ at zero bias [23] and increases almost symmetrically and linear with $V_1$ showing a pronounced downward kink at the gap edges $|V_1| = \Delta/e$ marked by vertical dashed lines. Above the gap the slope drops down consistent with the fact that transmission probability diminishes as soon as the quasiparticles can sink in the superconductor. Nonlocal noise is more informative than the usual two-terminal noise in NS structures [33, 41–43], which exhibits only a minor reduction in the presence of sub-gap density of states [44]. According to the equation (2), neglecting the contributions of $\mathcal{T}_-^2$ the slope $dS_2/dV_1$ is determined by $\mathcal{T}_+$ and allows to evaluate the linear response thermal conductance $G_{th} \equiv G_{th}^0 \Sigma\mathcal{T}_+$. We have $0.3 < G_{th}/G_{th}^0 < 1.6$, where $G_{th}^0 = \mathcal{L}Te^2/h$ is the thermal conductance quantum and $\mathcal{L}$ is the Lorenz number. This estimate of $G_{th}$ is legitimate provided $|\mathcal{T}_-| \ll 1$, i.e. if ballistic transmission is suppressed by disorder scattering [18, 45], as in our devices, or by structure geometry [46]. Note that our results manifest a drastic violation of the Wiedemann-Franz law [47] since a zero resistance of the NW region covered by the superconductor coexists with a relatively small thermal conductance via the sub-gap states.

Next we analyse the same data in terms of the nonlocal Fano factor, where the nonlocal current is obtained via $I_2 = -G_{22}V_2$. Here we use that the electric current caused by non-equilibrium quasiparticles is compensated by an extra current flowing in the opposite direction, so that the net current is zero in the floating configuration. This extra current flows near the Fermi level and is noiseless, since the junction $N_2$-NW-S remains essentially unbiased throughout the experiment, $|V_2| < k_BT/e$, see the Supplemental Material. Figures 3(c) and (d) plot $S_2$ vs $I_2$ for both devices. Two main features are evident. First, the symmetry inherent to $S_2$ vs $V_1$ data is in many cases lost here, since $I_2$ is not an anti-symmetric function of $V_1$. Second, the noise slope corresponds to nonlocal Fano factor values in the range $30 \lesssim F_{nl} \lesssim 100$, as shown by the dotted guide lines. Such giant values of $F_{nl}$ rule out a heretical interpretation that normal quasiparticle scattering from a poor quality Al/InAs interface is the main source of nonlocal signals, that would correspond to $F_{nl} \leqslant 1$, see the dashed guide line.

It is convenient to define the average charge of transmitted quasiparticles as the ratio between the transmitted charge and total number of transmitted quasiparticles $\langle q_T \rangle = \Sigma\mathcal{T}_-/\Sigma\mathcal{T}_+$. The value of $\langle q_T \rangle = 1$ corresponds to the case when quasiparticles conserve their charge during the transmission process, whereas in the case $\langle q_T \rangle = -1$ they invert the charge. As follows from the equations (1) and (2), $|\langle q_T \rangle| < 1/F_{nl}$, i.e. the observation of a giant Fano factor implies nearly charge-neutral nonlocal quasiparticle transport with $|\langle q_T \rangle| \ll 1$. This can be easily understood in case of a metallic diffusive NW covered by a superconductor with a transparent interface. Traversing the proximity region a quasiparticle experiences a number of ARs given on the average by $\langle N_{AR} \rangle = (w/d)^2$, where $w$ is the width of the S-terminal and $d \approx 100$ nm is the diameter of the NW. Given the randomness of diffusion the mean-square fluctuation is $\sqrt{\langle \delta N_{AR}^2 \rangle} = \sqrt{\langle N_{AR} \rangle} \geqslant 2$, so that the parity of $N_{AR}$ and thus the sign of the transmitted charge are completely uncertain. More rigorously, for the device NSN-II we find $|\langle q_T \rangle| < 0.01$, meaning that it takes at least a hundred quasiparticles to transmit a unit of elementary charge.

Our observations in a trivial superconducting phase have common features with the predicted nonlocal response at the topological phase transition in Majorana NWs. Here, even in presence of a moderate disorder, a finite transmission occurs in just one eigenchannel with $T_{21} = A_{21} = 1/4$ and results in a pure heat transport characterized by a universal peak of the thermal conductance $G_{th} = G_{th}^0/2$ [11]. While comparable in absolute value, $G_{th}$ in the present experiment demonstrates a monotonic dependence on $V_g$. The nonlocal charge response at the topological transition restores at a finite bias, $G_{21} \propto V_1$, owing to the energy-dependence of the transmission probabilities, known as the Andreev rectification [4]. Similar transport features are occasionally observable in figures 2(c) and (d), originating from mesoscopic fluctuations of $G_{21}$ around zero. This suggests that, unlike the peak in $G_{th}$, Andreev rectification is not a unique signature of the topological transition, see also [16].

As a final step, we demonstrate a crossover from nearly charge-neutral to normal nonlocal quasiparticle transport in

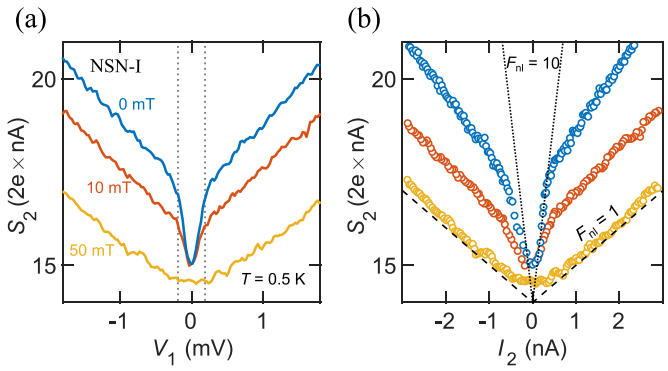


**Figure 4.** (a) Evolution of the nonlocal noise spectral density $S_2(V_1)$ in magnetic field and $T = 0.5$ K. Dotted lines show positions of the superconducting gap. (b) Evolution of the nonlocal noise spectral density $S_2(I_2)$ in magnetic field. Symbols have the same colour as the lines in panel (a) for the respective $B$. Guide lines with Fano-factor $F_{nl} = 1$ and $F_{nl} \gg 1$ are plotted as dashed and dotted lines correspondingly.

a magnetic field in the device NSN-I. Figure 4(a) shows the evolution of $S_2$ vs $V_1$, taken at a bath temperature of 0.5 K. The shot noise gradually diminishes at increasing $B$-field and the kink at the gap edge disappears concurrently with a transition of the Al to the normal state, see the $B = 50$ mT trace. Plotted as a function of $I_2$ in figure 4(b) this data reveals a transition from the giant noise at sub-gap energies in the $B = 0$ superconducting state to the Poissonian noise in the normal state, see the dashed guide line. In $B = 0$ we find $F_{nl} \sim 10$, considerably diminished compared to figure 3(c) as a result of thermal smearing. The Poissonian noise $F_{nl} \approx 1$ in the normal state corresponds to $A_{21} = 0$ and $T_{21} \ll 1$, as a result of residual interface scattering. Notably, in the superconducting state the slope corresponds to $F_{nl} > 1$ even beyond the kink, see also figures 3(c) and (d), since the probability of the AR remains finite above the gap [19].

In summary, we performed nonlocal transport and noise experiments in InAs NW-based hybrid NSN devices. Such a combination of all-electrical measurements allows to estimate the thermal conductance and reveals a predominantly charge-neutral origin of the nonlocal response. We expect that our approach will be generally useful for the studies of non-equilibrium proximity superconductivity, including unequivocal identification of the topological phase transition in Majorana devices.

We are grateful to A P Higginbotham, T M Klapwijk, A S Mel'nikov and K E Nagaev for helpful discussions. This work was financially supported by the RSF project 19-12-00 326 (fabrication, experiments in NSN-I device) and RFBR project 19-02-00 898 (experiments in NSN-II device). Theoretical framework was developed under the state task of the ISSP RAS. Work at TUM was supported by the Deutsche Forschungsgemeinschaft (DFG) via project KO-4005/5-1 and Germany's Excellence Strategy-EXC-2111-390814868 (Munich Center for Quantum Science and Technology, MCQST).

## Data availability statement

The data generated and/or analysed during the current study are not publicly available for legal/ethical reasons but are available from the corresponding author on reasonable request.

## ORCID iDs

S U Piatrusha https://orcid.org/0000-0003-3186-5608
A G Nasibulin https://orcid.org/0000-0002-1684-3948
G Koblmüller https://orcid.org/0000-0002-7228-0158
V S Khrapai https://orcid.org/0000-0002-1053-9654

## References

[1] den Hartog S G, Kapteyn C M A, van Wees B J, Klapwijk T M and Borghs G 1996 Transport in multiterminal normal-superconductor devices: reciprocity relations, negative and nonlocal resistances and reentrance of the proximity effect *Phys. Rev. Lett.* **77** 4954
[2] Lee G-H, Huang K-F, Efetov D K, Wei D S, Hart S, Taniguchi T, Watanabe K, Yacoby A and Kim P 2017 Inducing superconducting correlation in quantum hall edge states *Nat. Phys.* **13** 693
[3] Deng M-T, Vaitiekėnas S, Prada E, San-Jose P, Nygård J, Krogstrup P, Aguado R and Marcus C M 2018 Nonlocality of majorana modes in hybrid nanowires *Phys. Rev.* B **98** 085125
[4] Rosdahl T O, Vuik A, Kjaergaard M and Akhmerov A R 2018 Andreev rectifier: a nonlocal conductance signature of topological phase transitions *Phys. Rev.* B **97** 045421
[5] Lai Y-H, Sau J D and Das Sarma S 2019 Presence versus absence of end-to-end nonlocal conductance correlations in majorana nanowires: majorana bound states versus Andreev bound states *Phys. Rev.* B **100** 045302
[6] Danon J, Hellenes A B, Hansen E B, Casparis L, Higginbotham A P and Flensberg K 2020 Nonlocal conductance spectroscopy of Andreev bound states: symmetry relations and BCS charges *Phys. Rev. Lett.* **124** 036801
[7] Pan H, Sau J D and Sarma S D 2021 Three-terminal nonlocal conductance in majorana nanowires: distinguishing topological and trivial in realistic systems with disorder and inhomogeneous potential *Phys. Rev. B* **103** 014513
[8] Zhao L *et al* 2020 Interference of chiral Andreev edge states *Nat. Phys.* **16** 862–7
[9] Lutchyn R M, Sau J D and Das Sarma S 2010 Majorana fermions and a topological phase transition in semiconductor-superconductor heterostructures *Phys. Rev. Lett.* **105** 077001
[10] Oreg Y, Refael G and von Oppen F 2010 Helical liquids and majorana bound states in quantum wires *Phys. Rev. Lett.* **105** 177002
[11] Akhmerov A R, Dahlhaus J P, Hassler F, Wimmer M and Beenakker C W J 2011 Quantized conductance at the majorana phase transition in a disordered superconducting wire *Phys. Rev. Lett.* **106** 057001
[12] Mourik V, Zuo K, Frolov S M, Plissard S R, Bakkers E P A M and Kouwenhoven L P 2012 Signatures of majorana fermions in hybrid superconductor-semiconductor nanowire devices *Science* **336** 1003
[13] Das A, Ronen Y, Most Y, Oreg Y, Heiblum M and Shtrikman H 2012 Zero-bias peaks and splitting in an

Al-InAs nanowire topological superconductor as a signature of majorana fermions *Nat. Phys.* **8** 887 E
[14] Yu P, Chen J, Gomanko M, Badawy G, Bakkers E P A M, Zuo K, Mourik V and Frolov S M 2021 Non-majorana states yield nearly quantized conductance in superconductor-semiconductor nanowire devices *Nat. Phys.* **17** 482
[15] Ménard G C *et al* 2020 Conductance-matrix symmetries of a three-terminal hybrid device *Phys. Rev. Lett.* **124** 036802
[16] Puglia D, Martinez E A, Ménard G C, Pöschl A, Gronin S, Gardner G C, Kallaher R, Manfra M J, Marcus C M, Higginbotham A P and Casparis L 2021 Closing of the induced gap in a hybrid superconductor-semiconductor nanowire *Phys. Rev. B* **103** 235201
[17] Andreev A F 1964 Thermal conductivity of the intermediate state of superconductors *Zh. Eksp. Teor. Fiz.* **46** 1823
[18] Kopnin N B, Mel'nikov A S and Vinokur V M 2004 Reentrant localization of single-particle transport in disordered Andreev wires *Phys. Rev.* B **70** 075310
[19] Tinkham M 2004 *Introduction to Superconductivity* (*Introduction to Superconductivity*) (Mineola, New York: Dover Publications)
[20] Heikkilä T T, Silaev M, Virtanen P and Bergeret F S 2019 Thermal, electric and spin transport in superconductor/ferromagnetic-insulator structures *Prog. Surf. Sci.* **94** 100540
[21] Tikhonov E S, Shovkun D V, Ercolani D, Rossella F, Rocci M, Sorba L, Roddaro S and Khrapai V S 2016 Local noise in a diffusive conductor *Sci. Rep.* **6** 30621 E
[22] Claughton N R and Lambert C J 1996 Thermoelectric properties of mesoscopic superconductors *Phys. Rev.* B **53** 6605
[23] Anantram M P and Datta S 1996 Current fluctuations in mesoscopic systems with andreev scattering *Phys. Rev.* B **53** 16390
[24] Giazotto F, Heikkilä T T, Luukanen A, Savin A M and Pekola J P 2006 Opportunities for mesoscopics in thermometry and refrigeration: physics and applications *Rev. Mod. Phys.* **78** 217
[25] Chandrasekhar V 2009 Thermal transport in superconductor/normal-metal structures *Supercond. Sci. Technol.* **22** 083001
[26] Peltonen J T, Virtanen P, Meschke M, Koski J V, Heikkilä T T and Pekola J P 2010 Thermal conductance by the inverse proximity effect in a superconductor *Phys. Rev. Lett.* **105** 097004
[27] Bagrets D, Altland A and Kamenev A 2016 Sinai diffusion at quasi-1d topological phase transitions *Phys. Rev. Lett.* **117** 196801
[28] Tikhonov E S, Denisov A O, Piatrusha S U, Khrapach I N, Pekola J P, Karimi B, Jabdaraghi R N and Khrapai V S 2020 Spatial and energy resolution of electronic states by shot noise *Phys. Rev.* B **102** 085417
[29] Larocque S, Pinsolle E, Lupien C and Reulet B 2020 Shot noise of a temperature-biased tunnel junction *Phys. Rev. Lett.* **125** 106801
[30] Landauer R and Martin T 1991 Equilibrium and shot noise in mesoscopic systems *Physica* B **175** 167
[31] Blanter Y and Büttiker M 2000 Shot noise in mesoscopic conductors *Phys. Rep.* **336** 1
[32] Hofstetter L, Csonka S, Nygård J and Schönenberger C 2009 Cooper pair splitter realized in a two-quantum-dot y-junction *Nature* **461** 960
[33] Das A, Ronen Y, Heiblum M, Mahalu D, Kretinin A V and Shtrikman H 2012 High-efficiency cooper pair splitting demonstrated by two-particle conductance resonance and positive noise cross-correlation *Nat. Commun.* **3** 1165 E
[34] Deng M T, Vaitiekenas S, Hansen E B, Danon J, Leijnse M, Flensberg K, Nygård J, Krogstrup P and Marcus C M 2016 Majorana bound state in a coupled quantum-dot hybrid-nanowire system *Science* **354** 1557
[35] Albrecht S M, Higginbotham A P, Madsen M, Kuemmeth F, Jespersen T S, Nygård J, Krogstrup P and Marcus C M 2016 Exponential protection of zero modes in majorana islands *Nature* **531** 206
[36] Denisov A O, Bubis A V, Piatrusha S U, Titova N A, Nasibulin A G, Becker J, Treu J, Ruhstorfer D, Koblmueller G, Tikhonov E S, and Khrapai V S 2020 Heat-mode excitation in a proximity superconductor (arXiv:2006.09803)
[37] Ford A C, Ho J C, Chueh Y-L, Tseng Y-C, Fan Z, Guo J, Bokor J and Javey A 2009 Diameter-dependent electron mobility of InAs nanowires *Nano Lett.* **9** 360
[38] Lachenmann S G, Friedrich I, Förster A, Uhlisch D and Golubov A A 1997 Charge transport in superconductor/semiconductor/normal-conductor step junctions *Phys. Rev.* B **56** 14108
[39] Courtois H, Charlat P, Gandit P, Mailly D and Pannetier B 1999 *J. Low Temp. Phys.* **116** 187
[40] Beenakker C W J 1997 Random-matrix theory of quantum transport *Rev. Mod. Phys.* **69** 731
[41] Jehl X, Sanquer M, Calemczuk R and Mailly D 2000 Detection of doubled shot noise in short normal-metal/superconductor junctions *Nature* **405** 50
[42] Kozhevnikov A A, Schoelkopf R J and Prober D E 2000 Observation of photon-assisted noise in a diffusive normal metal–superconductor junction *Phys. Rev. Lett.* **84** 3398
[43] Choi B-R, Hansen A E, Kontos T, Hoffmann C, Oberholzer S, Belzig W, Schönenberger C, Akazaki T and Takayanagi H 2005 Shot-noise and conductance measurements of transparent superconductor/two-dimensional electron gas junctions *Phys. Rev.* B **72** 024501
[44] Tikhonov E S, Shovkun D V, Snelder M, Stehno M P, Huang Y, Golden M S, Golubov A A, Brinkman A and Khrapai V S 2016 Andreev reflection in an *s*-type superconductor proximized 3D topological insulator *Phys. Rev. Lett.* **117** 147001
[45] Haim A and Stern A 2019 Benefits of weak disorder in one-dimensional topological superconductors *Phys. Rev. Lett.* **122** 126801
[46] Laeven T, Nijholt B, Wimmer M and Akhmerov A R 2020 Enhanced proximity effect in zigzag-shaped majorana Josephson junctions *Phys. Rev. Lett.* **125** 086802
[47] Franz R and Wiedemann G 1853 Ueber die wärme-leitungsfähigkeit der metalle *Ann. Phys. Chem.* **165** 497